

A Lattice Boltzmann Approach to Wettability and Rate Effects on Relative Permeability using Digital Core Analysis

Louis K. Gbayan and Christoph H. Arns
University of New South Wales, Sydney, Australia

This paper was prepared for presentation at the International Symposium of the Society of Core Analysts held in Snowmass, Colorado, USA, 21-26 August 2016

ABSTRACT

Over the last decade digital rock physics has made significant advances in particular with regard to imaging technology including multi-scale imaging. In terms of transport property calculations from tomographic images physical properties related to single component fluids are reasonably well understood when the micro-structure is well resolved. The calculation of relative permeability remains challenging; fluid distributions at partial saturations are often obtained by direct imaging, rather than fluid flow simulation and calculations of relative permeability are carried out on the individual fluid partitions using a single phase lattice Boltzmann method (LBM) when considering systems of significant size. In this paper we use a lattice Boltzmann approach to simulate multi-component flow at typical wettability [1]. We base our simulations on the Shan and Chen lattice Boltzmann model for two phase flow. The degree of wetting was approximated by the contact angle between the wetting and non-wetting phase. We demonstrate the effect of discretization and initial conditions on the pressure field distribution. The Lattice Boltzmann model was validated against literature values for wetting and non-wetting contact angles. After this validation stage, the model was applied to reconstructed Fontainebleau sandstone where we can control image resolution.

INTRODUCTION

The Lattice Boltzmann method (LBM) is known to produce macroscopic behaviour of fluids by simulating the dynamics of particle ensembles on a regular lattice. The local nature of the computations and the easy implementation of boundary conditions make it particularly suitable for simulations on rock micro-structure and for multi-phase flow [2]. Various LBMs have been developed and applied to simulate real life phenomenon in different fields with varying degrees of accuracy and stability [3]. LBM models are known to be limited in their abilities to model fluid dynamics behaviour with regard to density ratios and viscosity ratios [3]. A particular question less researched is the effect of initial fluid distributions on final fluid distributions. Here we implement a Shan and Chen type LBM and a two relaxation time (TRT) approach to improve stability and accuracy.

SAMPLES AND INITIAL SATURATION

To allow a controlled assessment of initial saturations including discretization effects, we consider in this work a reconstructed Fontainebleau sandstone. This sample has been characterised in detail in [4]. For our simulations we select resolutions of 3.66 μm and 1.83 μm . Initial saturations are set using distance maps; namely the Euclidean distance transform (EDT), the covering radius transform (CRT), and the capillary drainage transform (CDT) [5,6]. We note that distances of EDT and CRT are local to a pore, as opposed to the CDT, which considers the connectivity of the pore space: the CRT assigns each voxel the radius of the largest sphere which can cover it, while the CDT applies the additional condition that this sphere has to be able to intrude from the physical boundary of the sample. The initial saturation distributions for the simulations are given in Fig. 1a-c; a particular saturation is set by applying a radius cut-off on the respective distance map. Here the resulting saturations are very similar, e.g. $S_w=53.2\%$ for CDT, $S_w=53.0\%$ for CRT, and $S_w=53.1\%$ for EDT for the high-resolution discretization. To avoid boundary errors in the calculations, the saturation maps were calculated on double the domain size used for flow calculations and the central 400^3 or 200^3 region selected and mirrored in flow direction for simulation of fluid flow. In all fluid flow simulations we consider the same field of view, which is 200^3 voxels (3.66 μm resolution) or 400^3 voxels (1.83 μm resolution) respectively.

LATTICE BOLTZMANN METHOD

The lattice Boltzmann model is a mesoscopic numerical scheme based on a simple collide and stream algorithm. We use a Shan and Chen type lattice Boltzmann based on various accuracy improving strategies and follow the implementation of [7,2]. The LBM evolution equation is given by

$$f_a^\sigma(\mathbf{x} + \mathbf{e}_a \Delta x, t + \delta t) - f_a^\sigma(\mathbf{x}, t) = f_{eqa}^\sigma(\mathbf{x}, t) - f_a^\sigma(\mathbf{x}, t) / \tau_\sigma \quad (1)$$

with position \mathbf{x} , time t , lattice directions \mathbf{e}_a , distribution function $f_a^\sigma(\mathbf{x}, t)$, equilibrium function $f_{eqa}^\sigma(\mathbf{x}, t)$, and relaxation time τ_σ , where σ denotes the fluid components. The equilibrium equation above is solved using the formulation below:

$$f_a^\sigma(\mathbf{x}, t) = w_a \rho^\sigma \left[1 + \mathbf{e}_a \cdot \frac{\mathbf{u}_\sigma^{eq}}{c_s^2} + \frac{(\mathbf{e}_a \cdot \mathbf{u}_\sigma^{eq})^2}{2c_s^4} - \frac{(\mathbf{u}_\sigma^{eq})^2}{2c_s^2} \right] \quad (2)$$

with equilibrium velocity \mathbf{u}_σ^{eq} . The macroscopic quantities of mass and velocities are calculated directly from there microscopic ones as:

$$\rho^\sigma = \sum_a f_a^\sigma \quad , \text{ and} \quad (3)$$

$$\rho^\sigma \mathbf{u}_\sigma^{eq} = \sum_a f_a^\sigma \mathbf{e}_a \quad . \quad (4)$$

Here ρ^σ is the density of component σ . Further implementation details can be found in [7,2]. We apply a half way bounce back boundary condition at the solid-fluid boundary. At the inlet and outlet, we mirror our image to achieve periodicity. Given the periodicity

of our domain, we apply a body force according to [7] to force each fluid. The definition of the adhesion/cohesion forces also follows [7,2]. The actual values are reported in the Figure captions.

To improve accuracy and stability of our LBM implementation, we use the TRT method as a special case of a multi-relaxation time (MRT) LBM. In the MRT relaxation rates are considered a diagonal matrix and are typically optimized for stability, conserved quantities, and accuracy. In the two relaxation time approach, the matrix reduces to two relaxation rates. Symmetric moments are relaxed with a particular choice of relaxation parameters and anti-symmetric ones are relaxed with a different one [8-10]. The optimization of these relaxation rates is not trivial particularly in a 2-phase flow simulation. It has been shown in [8] that the product of these relaxation times in the TRT $(1/s^+ - 1/2) \times (1/s^- - 1/2)$ depends on the heterogeneity of the sample structure.

RESULTS AND DISCUSSION

Figure 2 depicts high-resolution simulations of fluid distribution evolutions from three different initial saturation conditions set by the CDT, CRT, EDT respectively. Initial saturations across the whole domain are comparable. Two different contact angles of $\theta = 76.8^\circ$ and $\theta = 35.0^\circ$ are considered. The latter values is given in [1] for the case of water-wet Bentheimer sandstone, which is like Fontainebleau a rather clean water-wet sandstone. For contrast we added the case of high contact angle. Comparing the initial conditions (Fig. 1) to the LBM saturation evolution, it is clear that fluid configurations after 20,000 iterations are close to the initial conditions for the CDT and CRT. The EDT condition is less stable and approaches a saturation distribution similar to the CRT. We consider this a result of the local definition of distances (ordinary percolation) compared to the invasion percolation represented by the CDT. Furthermore, the EDT may initially provide good connectivity of both phases, while at the same time the sharp angles of the initial fluid distribution are unphysical. Comparing the rows [a-c] and [d-f] in Figure 2, we notice the clear difference in contact angle. It is apparent that the establishment of curvatures obeying contact angle settings in the simulation is relatively fast compared to approaching global equilibrium saturations—e.g., we expect that at equilibrium Fig.2d-f would show the same fluid saturation distribution, while actually after 20,000 iterations the initial saturation distribution is still visible. To explore resolution effects and consider longer simulation times, we reduced the lattice resolution by a factor of two in Figure 3. Time step $N=10,000$ in Figure 3.a corresponds to $N=20,000$ in Figure 2d-f. There is excellent agreement with local fluid distributions at this discretization level. Figure 3 illustrates that the convergence to global equilibrium fluid distributions is slow. It is noticeable that the fluid distributions are converging from $N=0$ (initial condition) to $N=80,000$; an order of magnitude step would be required to actually equilibrate fluids fully. We tested a further reduction in resolution to speed up the simulation. At that discretization level the evolution of fluid distributions diverged significantly with simulations at higher resolution.

CONCLUSION

We presented an implementation of a multi-relaxation time (MRT) method, which was applied for the particular case of two relaxation times (TRT). Multiple fluid distributions for initialisation of the simulations were considered. It is clear that initial fluid distributions have a strong impact on the fluid evolution pattern. In particular, there is a very pronounced difference in initial conditions between CDT and CRT. Initialisation using the EDT appears to be similar to the CRT and also has little physical basis, thus may be discarded. In the future we will be extending the current MRT LBM to include free energy and colour gradient approaches. It is clear that application of the LBM technique to heterogeneous porous media would require high stability and computational efficiency at the same time to address representative volumes. A different route may be the combination of micro-CT fluid distribution imaging with LBM fluid relaxation techniques e.g. to consider contact angle changes and their influence on petrophysical properties.

ACKNOWLEDGEMENTS

CHA acknowledges the ANU/UNSW Digital Core Consortium, the Australian Research Council (ARC) for a Future Fellowship, and the National Computing Infrastructure for generous allocation of computing time.

REFERENCES

1. T. Ramstad, P.E. Oren, S. Bakke, 2009, *Society of Petroleum Engineers*, SPE124617.
2. H. Huang, L. Wang, X-Y. Lu, 2011, *Comput. Math. Appl.*, **61**, 3606-3617.
3. E.S. Boek, M. Venturoli, 2011, *Comput. Math. Appl.*, **59**, 2303 – 2314.
4. D.E. Latief, B. Biswal, U. Fauzi, R. Hilfer, 2010, *Physica A*, **389**, 1607-1618.
5. M. Hilpert, C. T. Miller, 2001, *Adv. Wat. Res.*, **24**, 243.
6. C.H. Arns, M.A. Knackstedt, N.S. Martys, 2005, *Phys. Rev. E*, **72**, 046304.
7. N.S. Martys, H. Chen, 1996, *Phys. Rev. E*, **53**(1), 743-751.
8. L. Talon, D. Bauer, N. Gland, S. Youssef, H. Auradou, I. Ginzburg, 2012, *Wat. Res. Res.*, **48**(4), W04526.
9. A. Kuzmin, I. Ginzburg, A.A. Mohammed, 2011, *Comput. Math. Appl.*, **61**, 3417-3442.
10. I. Ginzburg, F. Verhaeghe, D. d'Humières, 2008, *Comm. Comp. Phys.*, **3**(2) 427-478.

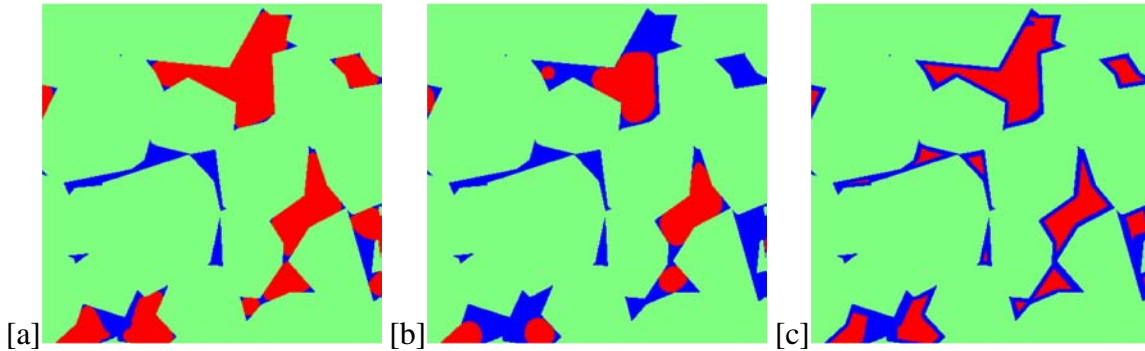


Fig.1: Slices through the initial saturation conditions for simulations on reconstructed Fontainebleau sandstone (subvolumes of 400^3 voxel). [a] Capillary drainage transform ($S_w=53.2\%$), [b] covering radius transform ($S_w=53.0\%$), [c] Euclidean distance map ($S_w=53.1\%$). Saturations are given for the full domain.

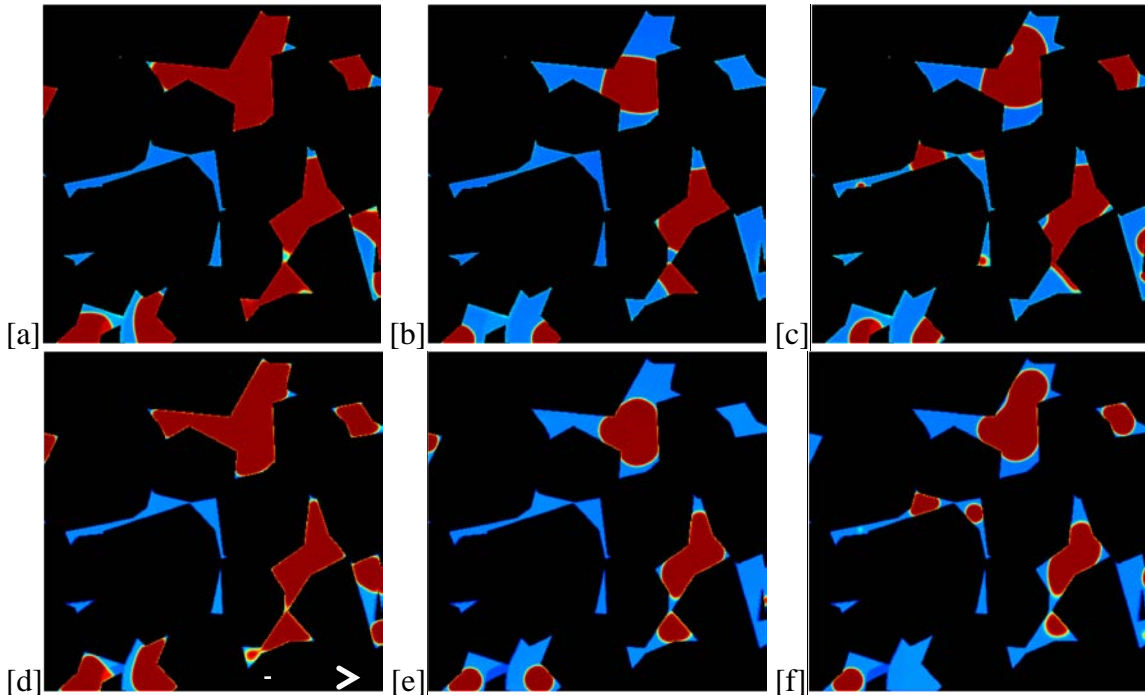


Fig.2: Slices through the density map of component one for LBM TRT simulations on reconstructed Fontainebleau sandstone corresponding to Fig. 1 (mirrored simulation domain $800 \times 400 \times 400$). Depicted are saturations after 20,000 iterations. [a-c]: $G_a = \pm 0.1$ corresponding $\theta = 76.8^\circ$. [d-f] $G_a = \pm 0.3769$ corresponding $\theta = 35.0^\circ$, $G_c = 1.35$, $\rho_{\text{initial}} = 4/3$ in the fluids and 0.04 of ρ_{initial} in the opposite fluid phase; $\tau_i = 1$ where $i=1,2$ are the fluid components, $F_a = \rho_{\text{initial}} \cdot 10^{-5}$ for both fluids in x-direction (white arrow).

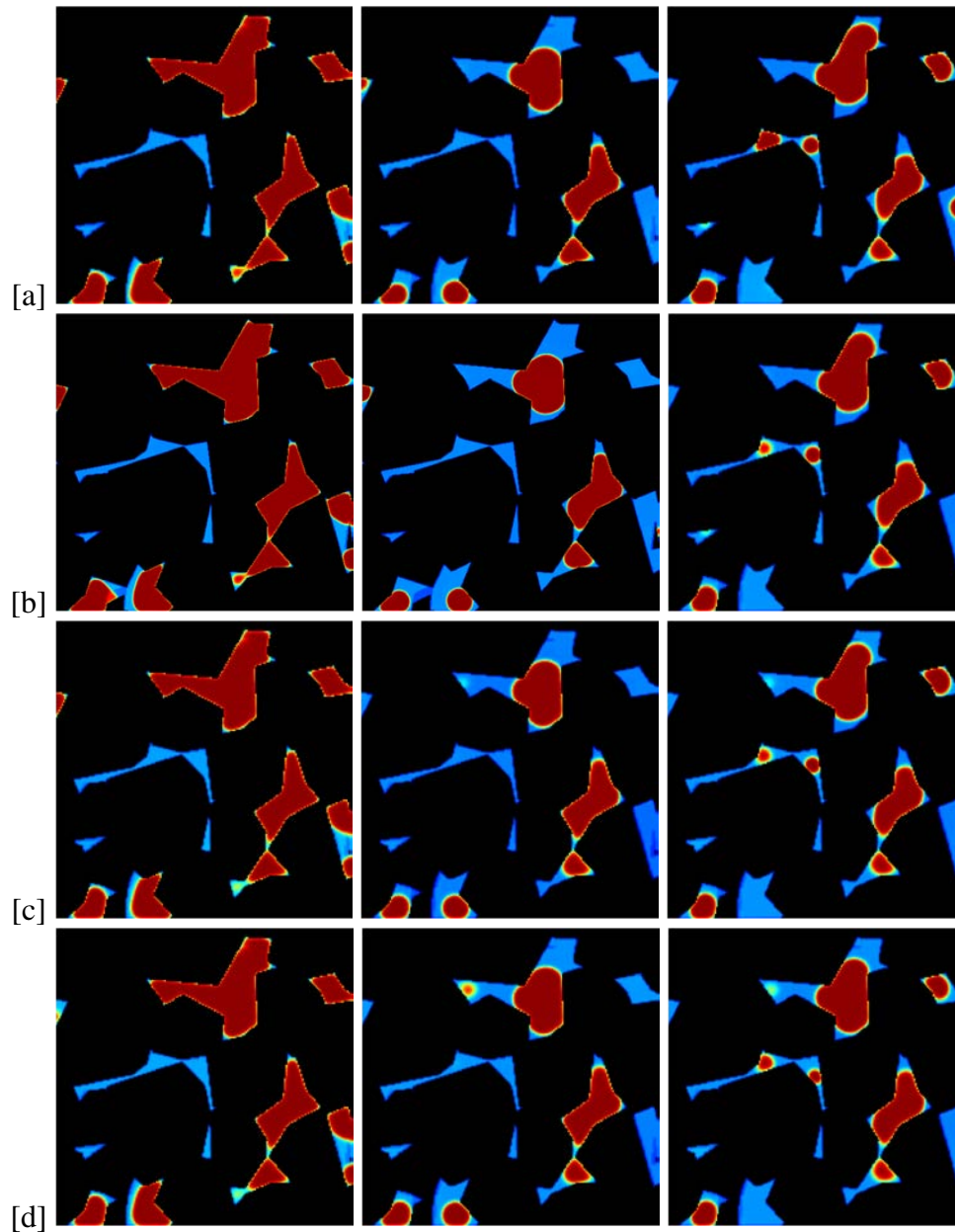


Fig.3: Slices through a time series of density maps with the same initial conditions as Fig. 2 at reduced resolution, but identical field of view (simulation domain $400 \times 200 \times 200$). *Left column*: initialisation by capillary drainage, *middle*: initialisation by covering radius, *right*: initialisation by Euclidean distance. Each row corresponds to a particular number of N iterations. [a]: $N=10,000$ (see corresponding time-step $N=20,000$ in Fig.2d-f), [b]: $N=20,000$, [c]: $N=40,000$, [d]: $N=80,000$. Physical properties are as in Fig. 2, [d-f].